

phys. stat. sol. (a) 176, 453 (1999)

Subject classification: 68.75.+x; 61.72.Lk; 68.35.Dv; S7.14

Dislocation Reduction in AlN and GaN Bulk Crystals Grown by HVPE

M. ALBRECHT (a), I.P. NIKITINA (b), A.E. NIKOLAEV (b), YU.V. MELNIK (b, c),
V.A. DMITRIEV (b, c, d), and H.P. STRUNK (a)

(a) *Institut für Werkstoffwissenschaften, Lehrstuhl Mikrocharakterisierung,
Universität Erlangen-Nürnberg, Cauerstr. 6, D-91058 Erlangen, Germany*

(b) *A.F. Ioffe Physico-Technical Institute, Wide Band Gap Research Group,
Politekhnicheskaya 26, 194021 St. Petersburg, Russia*

(c) *TDI, Inc., 8660 Dakota Dr., Grailersburg MD 20877, USA*

(d) *Materials Research Center of Excellence, School of Engineering, Howard University,
2300 Sixth St., NW Washington, DC 20059, USA.*

(Received July 4, 1999)

We analyse the dislocation distribution in GaN and AlN bulk crystals by transmission electron microscopy and X-ray diffraction. The crystals are grown by hydride vapour phase epitaxy onto 6H-SiC[0001] and Si(111) substrates. Two essentially different dislocation populations are observed: (i) a-type dislocations that show efficient dislocation density reduction (down to $4 \times 10^5 \text{ cm}^{-2}$) and (ii) a, (a + c) and c-type dislocations each type in a considerable density with less efficient dislocation reduction. We evaluate the dislocation processes that result in this different behaviour as dependent on the dislocation population.

1. Introduction

Single crystalline GaN substrates with low defect densities are nowadays grown by three different approaches: (i) growth from the solution at high pressures and high temperatures [1], (ii) masking of an epitaxial GaN layer with silicon dioxide or silicon nitride stripes and subsequent lateral epitaxial overgrowth [2, 3] and (iii) growth of thick GaN layers on either sapphire [4, 5] or SiC [5] and subsequent removal of the substrates. While material grown from solution is practically dislocation free, crystals grown on foreign substrates contain misfit dislocations induced by the lattice mismatch between substrate and layer. These misfit dislocations, when extending into the layer, form threading dislocations, that may affect electronical and optical properties. Moreover, high residual strains or even cracking may occur upon cooling to room temperature due to a difference in thermal expansion coefficients between substrate and overlayer [7 to 9].

Tackling these problems means firstly understanding the fundamental dislocation processes. While dislocation processes in heteroepitaxial cubic systems are well examined, up to now very few analogous work exists (e.g. [10 to 12]) for nitrides. In this work we analyse by means of transmission electron microscopy and X-ray diffraction some of the processes that take place in GaN and AlN crystals grown by hydride vapour phase epitaxy (HVPE) to thicknesses of 100 to 200 μm .

2. Experimental

2.1 Sample Growth

GaN and AlN epitaxial layers were grown up to 100 to 200 μm thickness by HVPE onto 6H-SiC(0001) and Si(111) substrates respectively (for details of the growth processes see [6]). The growth temperatures range from 1120 to 1320 K, the growth rate is about 0.06 mm/h. The SiC substrates were removed by reactive ion etching (RIE) in a SF_6 containing gas mixture to obtain free standing bulk GaN crystals (maximum size of $7 \times 6 \times 0.1 \text{ mm}^3$). Fracture of the layers was the main factor limiting the size of these bulk crystals. The responsible strains result from the lattice mismatch and different thermal expansion coefficients of GaN and SiC.

2.2 Characterisation

After removal of the substrate, the crystals were examined using double crystal X-ray spectrometer. We measure rocking curves (ω) and (ω , 2θ) scanning modes) at both sides of the bulk crystals (i.e. the former interface and the free surface). High quality 6H-SiC crystals were used as monochromator and analyser. We use both symmetric (0002) and asymmetric (11 $\bar{2}$ 4) reflections, and determine the residual strain in the layers to estimate the fraction between a-type ($b = 1/3\langle 11\bar{2}0 \rangle$) and a + c ($b = 1/3\langle 11\bar{2}0 \rangle$) and c-type ($b = \langle 0001 \rangle$) dislocations. A small FWHM of the (0002) reflection compared to that of the (11 $\bar{2}$ 4) reflection thus indicates a low density of dislocations with c-component (a + c, c).

Transmission electron microscopy measurements of plane-view and cross-sectional samples in a Philips CM 30 operating at 300 keV render detailed information on dislocations. We analyse areas close to the free surface and to the former interface (the maximum areas analysed were about 100 μm in diameter). Stereo microscopy aids the analysis of the spatial distributions, the glide geometry and of the details of dislocation interactions. TEM samples were prepared using conventional techniques including mechanical grinding, polishing and 4 keV Ar^+ ion milling using a liquid nitrogen cooling stage until electron transparency is reached.

3. Results

3.1 X-ray analysis

An example for an X-ray analysis of a high quality GaN crystal is summarised in Table 1. Three observations are most important: (i) the FWHM decreases from the inter-

Table 1
Full width at half maximum of rocking curves from a GaN bulk crystal grown by HVPE.
Cu-K α radiation

	ω -scan (0002) [arcsec]	ω -scan (11 $\bar{2}$ 4) [arcsec]	ω , 2θ -scan (0002) [arcsec]	ω , 2θ -scan (11 $\bar{2}$ 4) [arcsec]
Surface	91	110	19	100
Former interface	131	180	27	160

face to the surface in both reflections (in ω as well as in $(\omega, 2\theta)$ scans), (ii) the FWHM for $(\omega, 2\theta)$ scans of (0002) and (11 $\bar{2}$ 4) reflections are pronouncedly different (this holds for the free surface of the GaN crystal as well as for the former interface), (iii) the FWHM decreases from the former interface to the free surface and is more pronounced for the asymmetric reflections than for the symmetric ones in (ω) as well as in $(\omega, 2\theta)$ scans. These dependences lead to two main conclusions as concerns the dislocation distribution. The reduced FWHM of the symmetrical reflection indicates a low density of dislocations with c-component in this specific crystal as compared to a-dislocations (large FWHM of asymmetric reflection). Moreover, the density of a-type dislocations decreases more efficiently than that of dislocations with c-component.

AlN layers on Si(111) contain a high density of a+c and c-type threading dislocations as indicated by the large FWHM of the ω -scan (44.3 arcmin at the former interface, 38.4 arcmin at the free surface).

3.2 Dislocation analysis

A typical cross-sectional micrograph of GaN bulk samples close to the former interface can be seen in Fig. 1a. Contrast analyses show pure a-type and pure c-type threading dislocations to be present. Dislocations with a c-component have [0001] line directions and are thus pure screw dislocations. Their density is as low as $3 \times 10^6 \text{ cm}^{-2}$. The a-type dislocations occur in a density

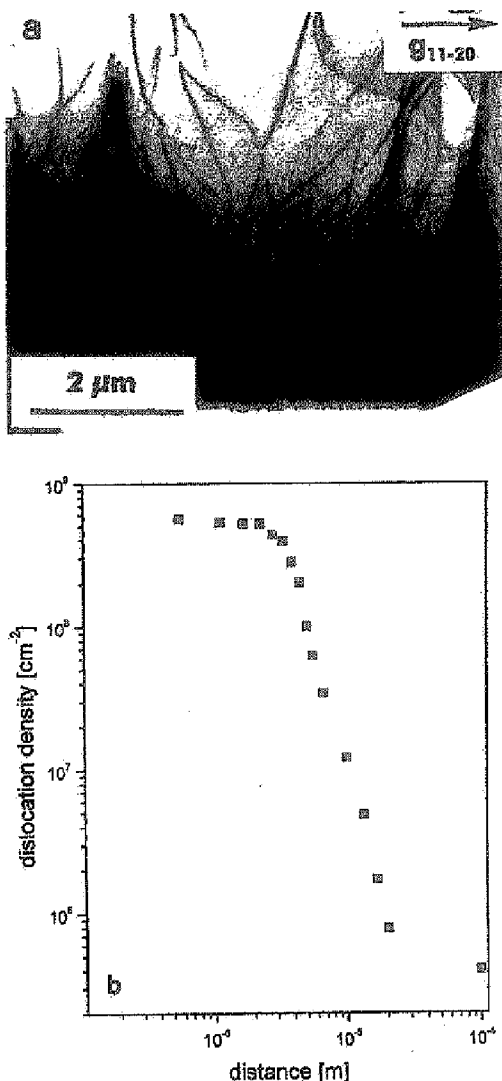


Fig. 1. Dislocation distribution in a 100 μm GaN crystal grown onto 6H-SiC(0001). a) Threading dislocations at the interface between a 200 μm thick GaN layer and the SiC substrate. Dislocations interact with each other by glide on prismatic and pyramidal glide planes. The interaction is due to the strain field of dislocations. Cross sectional transmission electron micrograph is taken under [11 $\bar{2}$ 0] multi-beam conditions. b) Dislocation density in HVPE grown GaN as dependent on the distance from the interface. The dislocation density reduces exponentially going from the interface to the free surface

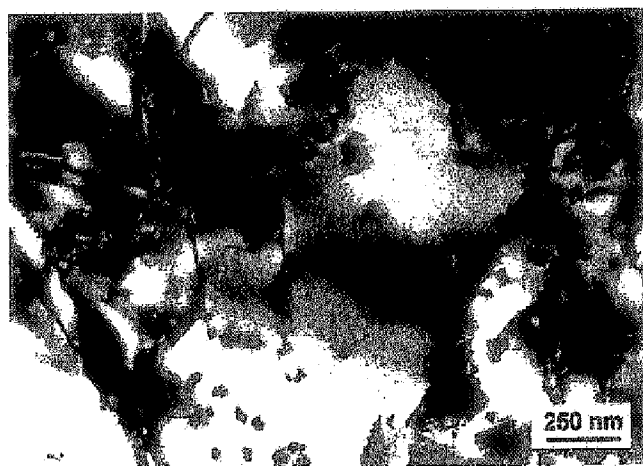


Fig. 2. Plane view of AlN crystal close to the growth surface. The dislocation density is $3.1 \times 10^8 \text{ cm}^{-2}$. Dislocations of different types (a, a + c, c-type) occur in comparable densities (see text)

of $8.3 \times 10^8 \text{ cm}^{-2}$. All these a-type dislocations lie inclined to the interface. Stereo microscopy revealed that a-type threading dislocations extend into prism ($\{1\bar{1}00\}$ -type) or pyramidal planes ($\{110\bar{1}\}$ type) thereby depositing a-type screw dislocations in the c-plane. Analysis points to essentially three different types of density reducing dislocation reactions: (i) $a - a \rightarrow 0$ (annihilation), (ii) $a_1 + a_2 \rightarrow a_3$ (recombination), (iii) $a + c \rightarrow (a + c)$. The dislocation density reduces exponentially in going away from the former interface to the free surface of the layer (dislocation density there: $4 \times 10^5 \text{ cm}^{-2}$) and large areas can be found that are completely free of dislocations. An evaluation of the dislocation density from TEM data as dependent on the depth is given in Fig. 1b.

AlN bulk crystals have an essentially different dislocation structure. Close to the former interface the density of threading dislocations is in the range between 10^9 to 10^{10} cm^{-2} . Threading dislocations are of a-type, c-type and (a + c)-type. According to plane-view micrographs threading dislocations are distributed randomly, not in small angle grain boundaries (Fig. 2). These threading dislocation align along $[0001]$ directions. A high density of stacking faults is also present. Close to the free surface the threading dislocation density is reduced to $3.1 \times 10^8 \text{ cm}^{-2}$, (a-type: $1.8 \times 10^8 \text{ cm}^{-2}$, a + c-type: $0.8 \times 10^8 \text{ cm}^{-2}$, c-type: $0.5 \times 10^8 \text{ cm}^{-2}$).

4. Discussion

Our structural analysis of AlN and GaN bulk crystals grown by HVPE suggests a correlation between dislocation population and dislocation density reduction we will briefly substantiate in the following in an appropriate way: (i) layers with predominantly a-type threading dislocations (notably GaN on SiC without buffer layer) exhibit an exponentially decreasing dislocation density from 10^9 cm^{-2} at the former interface to the free surface say $100 \mu\text{m}$ apart, to 10^5 cm^{-2} . (ii) Layers with a-type and a+c-type threading dislocations in comparable densities (e.g. AlN) show a drastically smaller degree of reduction in dislocation density near the free surface of thick layers (in contrast to case (i)).

In the following discussion we will put together a few arguments on the basis of dislocation formation and interaction to show that it is the type of dislocation population that leads to the varied efficiency in dislocation reduction.

We can model the observation of predominantly a-type dislocations in the case (i) by assuming only a-type dislocations to form during the initial stages of growth. Their Burgers vector are contained within the basal growth plane and these dislocations are rather efficient in compensating the misfit. Because of the high misfit GaN growth on SiC starts with island formation [13] and a-type misfit dislocations may form by glide from the rims of the individual islands along the interface. (Without loss of generality we can visualise it as a network made of 60° dislocations.) As the initial network may vary from island to island, the dislocations that do not find an immediate partner will, on island coalescence, bend over and form threading dislocations [14]. The analysis shows that these dislocations lie on prism and pyramidal planes. The interesting aspect now is that these planes are active glide planes [15]. As a consequence, the dislocations can glide together under the mutually exerted attractive strain fields and annihilate, when two dislocations with opposite Burgers vectors meet, or when two dislocations vectors a_1 and a_2 attract each other, to recombine to a dislocation with Burgers vector a_3 (see Section 3.2). This resulting dislocation of course, is available for a further recombination process and so on, until this sequence is stopped by an annihilation. The processes may occur irrespective of what glide planes are involved and thus are very efficient. Romanov et al. [16] have calculated that under these conditions (no dislocation blocking) the dislocation density decreases exponentially with thickness as observed.

Case (ii) is characterised by the fact that threading dislocations with a, (a + c) and c-type dislocations occur in similar densities in the HVPE layer. We can infer that the origin of this population lies again in the initial growth stage. If we assume a closed nearly two-dimensional growth at the beginning of GaN growth, plastic relaxation in the closed layer by a-type dislocations is indebted because no shear stresses are present to drive dislocations in the interface. Thus, other types of dislocations, especially (a + c)-type dislocations form in thick III-nitride layer, because these are the only ones that experience shear stress and can accommodate the mismatch [15]. From a detailed analysis of the 400 possible dislocation recombination and annihilation reactions ([17]), we can draw three main conclusions: (i) the additional c-component of the Burgers vector reduces the probability for dislocation annihilation from 0.5 (a-type dislocations reacting among each other) to 0.25 (a + c-type dislocations reacting among each other). (ii) the glide of (a + c)-type dislocations in prismatic and pyramidal planes is highly unfavourable compared to glide of a-type dislocations because of the Peierls force in these glide systems; (iii) The additional c-Burgers vector component leads to many pinning points because of the essentially three-dimensional network of dislocations. In consequence the possibilities for dislocation density reduction are strongly reduced. The dislocation density then stays at a high level as observed.

5. Conclusions

We have analysed different dislocation populations in HVPE GaN and AlN bulk crystals. These populations are controlled by the initial growth process which is determined about the Burgers vector selection. Our results show that these populations are linked to important aspects of bulk crystal properties. When only a-type dislocations are pre-

sent an efficient reduction mechanism reduces the dislocation density to $4 \times 10^5 \text{ cm}^{-2}$ or less. When the dislocations are distributed on all possible Burgers vectors in equal density (in the range 10^8 cm^{-2} each group) then only a small density reduction occurs (two orders of magnitude at $100 \mu\text{m}$). In consequence, it is a task of the future to analyse the initial growth stages with respect to the developing dislocation population and then to conduct growth such that positive aspects are combined, low dislocation density and no cracking.

Acknowledgements The authors gratefully acknowledge financial support by INTAS grant No 96-2131. Part of the TEM work has been performed at the "Verbundlabor Hochauflösende Elektronenmikroskopie", Erlangen.

References

- [1] M. LESZYNSKI, T. SUSKI, H. TEISSYRE, P. PERLIN, I. GRZEGORY, J. JUN, S. POROWSKI, and T.D. MOUSTAKAS, *J. Appl. Phys.* **76**, 4909 (1994).
- [2] Y. KATO, S. KITAMURA, K. HIRAMATSU, and N. SAWAKI, *J. Cryst. Growth* **144**, 133 (1994).
- [3] O.H. NAM, B. BREMSER, B. WARD, R. NEMANICH, and R.F. DAVIS, *Jpn. J. Appl. Phys.* **36**, L532 (1997).
- [4] T. DETCHPROM, K. HIRAMATSU, K. ITOH, and I. AKASAKI, *Jpn. J. Appl. Phys.* **31**, L1454 (1992).
- [5] R.J. MOLNAR, W. GÜTZ, L.T. ROMANO, and N.M. JOHNSON, *J. Cryst. Growth* **178**, 147 (1997).
- [6] YU.V. MELNIK, K. VASSILEVSKI, I.P. NIKITINA, A.I. BABANIN, V.YU. DAVIDOV, and V.A. DMITRIEV, *MRS Internet J. Nitride Semicond. Res.* **2**, art. No. 3 (1997).
- [7] N. ITOH, J.C. RHEE, T. KAWABATA, and S. KOIKE, *J. Appl. Phys.* **58**, 1828 (1985).
- [8] T. KOZAWA, T. KACHI, H. KANO, H. NAGASE, N. KOIDE, and K. MANABE, *J. Appl. Phys.* **77**, 4389 (1995).
- [9] I.P. NIKITINA, M.P. SHEGLOV, YU.V. MELNIK, K.G. IRVINE, and V.A. DMITRIEV, *Diamond and Related Mater.* **6**, 1524 (1997).
- [10] L.T. ROMANO, B.S. KURSÖR, and R.J. MOLNAR, *Appl. Phys. Lett.* **71**, 2283 (1997).
- [11] A. SAKAI, H. SUNAKAWA, and A. USUI, *Appl. Phys. Lett.* **71**, 2259 (1997).
- [12] V. FERREGOTTO, A. GEORGE, and J.-P. MICHEL, *Mater. Sci. Engng. A* **234/236**, 625 (1997).
- [13] V.A. DMITRIEV, K. IRVINE, A. ZUBRILOV, D. TSVETKOV, V. NIKOLAEV, M. KAKOBSON, D. NELSON, and A. STNIKOVA, *Mater. Res. Soc. Symp. Proc.* **395**, 295 (1996).
- [14] X.J. NING, F.R. CHIEN, P. PIROUZ, J.W. YANG, and M. ASIF KHAN, *J. Mater. Res.* **11**, 580 (1996).
- [15] B. JAHNEN, M. ALBRECHT, W. DORSCH, S. CHRISTIANSEN, H.P. STRUNK, D. HANSER, and R.F. DAVIS, *MRS Internet J. Nitride Semicond. Res.* **3**, Art.39 (1998).
- [16] A.E. ROMANOV, W. POMPE, S. MATHIS, G.E. BELTZ, and J.S. SPECK, *J. Appl. Phys.* **85**, 182 (1999).
- [17] M. ALBRECHT, I.P. NIKITINA, A.E. NIKOLAEV, YU.V. MELNIK, V.A. DMITRIEV, and H.P. STRUNK, submitted to *J. Appl. Phys.*